Available online at www.sciencedirect.com
ScienceDirect
C. R. Physique 10 (2009) 907–915
COMPTES RENDUS PHYSIQUE

Experimental determination of Boltzmann's constant

Precise determination of the Doppler width of a rovibrational absorption line using a comb-locked diode laser

Koichi M.T. Yamada [a,*], Atsushi Onae [b], Feng-Lei Hong [b], Hajime Inaba [b], Tadao Shimizu [b]

[a] *Institute for Environmental Management Technology (EMTech), AIST, Onogawa 16-1, Tsukuba 305-8569, Japan*
[b] *National Metrology Institute of Japan (NMIJ), AIST, Umezono 1-1-1, Tsukuba 305-8563, Japan*

Available online 20 November 2009

Abstract

We had reported in a previous paper the precision measurement of line profiles of a transition of ^{13}C acetylene in the near-infrared region, employing a tunable diode-laser spectrometer, the frequency of which is locked to an optical-comb signal [K.M.T. Yamada et al., J. Mol. Spectrosc. 249 (2008) 95–99]. In the present article we review the methodology for the experiment and the analysis in determining the Boltzmann constant from the Doppler width of a rovibrational transition on the basis of our experiences. Problems to be surmounted for further improvement in accuracy are discussed. ***To cite this article: K.M.T. Yamada et al., C. R. Physique 10 (2009).***

Résumé

Détermination expérimentale de la largeur Doppler d'une raie d'absorption moléculaire rovibrationnelle en utilisant une diode laser asservie à l'aide d'un peigne de fréquences. Dans un article précédent, nous avons publié les résultats obtenus pour l'observation du profil des raies d'une transition dans l'acétylène ^{13}C dans le proche infrarouge. Ce travail a été effectué en utilisant un spectrométre à diode laser accordable, la fréquence du signal étant pilotée à l'aide d'un peigne de fréquences optiques [K.M.T. Yamada et al., J. Mol. Spectrosc. 249 (2008) 95–99]. Dans le présent article nous décrivons la méthode expérimentale employée et nous approfondissons l'analyse permettant de déduire de nos résultats une détermination de la constante de Boltzmann k_B à partir de la largeur Doppler observée. Nous discutons également les difficultés restant à surmonter pour améliorer l'exactitude de la mesure de k_B. ***Pour citer cet article : K.M.T. Yamada et al., C. R. Physique 10 (2009).***

Keywords: Boltzmann constant; Doppler width; Acetylene; Frequency comb; NIR

Mots-clés : Constante de Boltzmann ; Largeur Doppler ; Spectroscopie IR ; Peigne de frequences ; Acétylène

* Corresponding author.
E-mail addresses: kmt.yamada@aist.go.jp (K.M.T. Yamada), a-onae@aist.go.jp (A. Onae), f.hong@aist.go.jp (F.-L. Hong), h.inaba@aist.go.jp (H. Inaba), tadao-shimizu@aist.go.jp (T. Shimizu).

1631-0705/$ – see front matter
doi:10.1016/j.crhy.2009.10.011

1. Introduction

The CODATA recommended value of the Boltzmann constant [1,2] is $k = 1.3806505(24) \times 10^{-23}\ \mathrm{J\,K^{-1}}$, which was determined from the speed of sound measured by using a spherical acoustic resonator with the relative uncertainty of 1.8 ppm. Although the Boltzmann constant is often expressed as k_B, we denote it simply by k in this paper. The Boltzmann constant is a fundamental constant, which is related to many observable quantities through the thermal average over the population for each state governed by the Boltzmann distribution law. Thus there may be other methods to measure it; additional measurements independent of the acoustic measurement are useful in all cases [3]. The high-resolution measurement of pure rotational and rovibrational spectra of molecules with high precision is a good candidate for that.

Primary information obtained from the high-resolution spectra is the line-center positions, which have been used to determine the molecular structure in a wide sense. In addition, carefully measured spectral line profiles provide also information of the intensity and the width for each line. The intensity and the width carry the thermodynamical information of the molecules in the sample cell, and the following quantities contain the information of the Boltzmann constant:

(i) relative intensity observed for the rotational structure,
(ii) relative intensity observed for vibrational satellites (*hot* bands),
(iii) the Doppler width of an individual line.

Among them the third one seems to be most promising in the sense of high precision, because it is essentially a frequency measurement; thanks to the advance in the modern technique the uncertainty of the frequency measurement reaches 10^{-15}.

In the early stage, Bordé had proposed the spectroscopic methods to determine the Boltzmann constant from the observed Doppler width [4,5] and presented, together with coworkers, the first results on a rovibrational transition of NH_3 in 10 μm region [6]. Using a sophisticated CO_2 laser-sideband spectrometer and a temperature-stabilized cell at the melting point of ice, they realized the uncertainty of 200 ppm. Being stimulated by their work, we tried to measure line profiles with high precision in the near infrared region, where precise measurements can be performed relatively easily, using a diode-laser spectrometer locked to an optical-comb signal [7].

The Doppler width originates from the velocity distribution of the molecules in the cell; in an ideal case the spectrum broadened by the Doppler effect is represented by the Gaussian profile following the Maxwell–Boltzmann distribution. From the experimental point of view, however, the observed line profile is not purely Gaussian in any realistic measurement by various reasons. Therefore, a proper handling of line profiles is required to deduce the Gaussian line width which is related to the Boltzmann constant.

In Section 2, the mathematical expression for the line profile is briefly reviewed. Our experimental procedure is presented in Section 3, the results of the line-profile analysis in Section 4, and in the last Section 5 the problems to be solved in the future are discussed.

2. Spectral line profiles

2.1. Lambert–Beer's law

For simplicity we consider a two-level-system, where each molecule has only two energy levels, level 1 (ground state) and level 2 (excited state). When a photon resonant with the energy difference of the two, $h\nu_0 = E_2 - E_1$, interacts with the molecule, molecules in the level 1 absorb the photon, with a certain probability, and are excited to the level 2. Contrarily, molecules in the level 2 emit photons of energy $h\nu_0$. The probability of the absorption and the emission is governed by Einstein's B coefficient. Since these processes occur even if the energy of the incident photon is not exactly resonant, and thus we observe a spectral line with a finite width.

When a sample cell is irradiated with monochromatic light of frequency ν, the transmitted power of the radiation $I(\nu)$ is expressed by Lambert–Beer's law, i.e.

$$I(\nu) = I_0(\nu) \exp\bigl[-\sigma P(\nu, \nu_0)\bigr] \tag{1}$$

where $I_0(\nu)$ is the incident power of radiation, σ the intensity factor, and $P(\nu, \nu_0)$ the profile function. The intensity factor depends on the Einstein B coefficient, the number of the molecules in the level 1 and 2, and the length of the cell containing the molecules. The profile function $P(\nu, \nu_0)$ may be a Gaussian function, a Lorentzian function, a Voigt function, and etc. as discussed in the following.

2.2. The Doppler shift and the Doppler broadening

In gas phase experiments, the spectral lines are broadened inhomogeneously by the Doppler effect. The resonance frequency of each molecule is shifted by the Doppler effect:

$$\nu = \nu_0(1 + v_Z/c) \tag{2}$$

where ν is the Doppler shifted resonance frequency, ν_0 is the resonance frequency at the rest, v_Z is the component of velocity vector of the molecule in the incident direction of radiation, and c is the speed of light. Assuming the Maxwell–Boltzmann distribution in the thermal equilibrium at a temperature T, the fraction of molecules which moves with the velocity component v_Z is given by

$$w(v_Z) = \exp\bigl[-Mv_Z^2/(2kT)\bigr] \tag{3}$$

where M is the mass of the molecule. Using Eq. (2) v_Z in the equation can be replaced by the Doppler shift $\nu - \nu_0$, and we have

$$w(\nu - \nu_0) = \exp\bigl[-Mc^2(\nu - \nu_0)^2/\bigl(2\nu_0^2 kT\bigr)\bigr] = \exp\left[-\left(\frac{\nu - \nu_0}{\Gamma_{\mathrm{G}}}\right)^2\right] \tag{4}$$

which is a Gaussian distribution function, and

$$\Gamma_{\mathrm{G}} = \frac{\nu_0}{c}\sqrt{\frac{2kT}{M}} \tag{5}$$

is the half-width at $(1/e)$ maximum (denoted hereafter as HWM/e) of the Gaussian distribution.

The line profile, observed as a sum of the contribution from each molecule in the cell, is thus broadened by the Doppler effect. The Doppler broadened line profile is expressed by a Gaussian function $g(\nu, \nu_0)$:

$$g(\nu, \nu_0) = \frac{1}{\sqrt{\pi}\,\Gamma_{\mathrm{G}}}\exp\left[-\left(\frac{\nu - \nu_0}{\Gamma_{\mathrm{G}}}\right)^2\right] \tag{6}$$

Thus, if the line profile is purely Gaussian, Eq. (6), we can derive the Boltzmann constant k from the observed Γ_{G} provided that the temperature of the cell is known, because the other parameters, ν_0, M, and c, in Eq. (5) should be known with enough accuracy. The value of Γ_{G} is related to the Doppler width Δ_{D}, which is usually defined as the half-width at half-maximum (HWHM), by $\Delta_{\mathrm{D}} = \sqrt{\ln 2}\Gamma_{\mathrm{G}}$.

From the experimental point of view, it is impossible to realize the experimental condition where the line profile is purely Gaussian, because of the contribution of the homogeneous broadening as discussed next.

2.3. Homogeneous broadening and the Voigt profile

The line profile is broadened not only by the Doppler effect. The quantum state of a molecule can be observed only for a finite period of time by various reasons, such as the natural life time. If we observe the energy of a state over a period of τ, the observed energy must be uncertain by the amount of $\Delta E \approx \hbar/\tau$.

This uncertainty due to the finite observation time results in the line broadening, common to all molecules in concern; thus this broadening is called *homogeneous* broadening. The homogeneously broadened line profile is expressed by a Lorentzian function $f(\nu, \nu_0)$:

$$f(\nu, \nu_0) = \frac{1}{\pi}\frac{\Delta_{\mathrm{L}}}{(\nu - \nu_0)^2 + \Delta_{\mathrm{L}}^2} \tag{7}$$

where Δ_{L} is the half-width at half-maximum (HWHM) of the Lorentzian function. In usual experimental conditions, the homogeneous broadening is caused primarily by the collisional effect, i.e. the pressure broadening, which depends on the sample pressure linearly in a good approximation, i.e.

$$\Delta_{\mathrm{L}} = \Delta_{\mathrm{p}} = \gamma_{\mathrm{p}} p \tag{8}$$

where γ_p is the pressure broadening coefficient and p is the sample pressure. The other origins of the homogeneous broadening will be discussed in Section 5.

Since the line profile of each molecule, the resonance frequency of which is Doppler shifted as described Section 2.2, is homogeneously broadened, we observe the line profile in the gas phase as a convolution of the Gaussian and Lorentzian functions. The resultant profile function is called "Voigt profile", $V(\nu, \nu_0)$:

$$V(\nu, \nu_0) = \int_{-\infty}^{+\infty} f(\nu, \nu_1) g(\nu_1, \nu_0)\, \mathrm{d}\nu_1 = \frac{\Delta_L}{\pi^{3/2} \Gamma_G} \int_{-\infty}^{+\infty} \frac{\exp[-(\nu - \nu_1)^2/\Gamma_G^2]}{(\nu_1 - \nu_0)^2 + \Delta_L^2}\, \mathrm{d}\nu_1 \tag{9}$$

The Gaussian width Γ_G and the Lorentzian width Δ_L in Eq. (9) can be determined from an observed line profile by using a proper fitting procedure. If Γ_G obtained by the fit has the physical meaning defined by Eq. (8), the Boltzmann constant k can be readily derived from Γ_G and the temperature T of the sample. It is, however, not the case. The values of Γ_G obtained by fitting observed profiles are usually less than that predicted by Eq. (5) due to the collisional narrowing effect discussed next.

2.4. Collisional narrowing

The Gaussian width, Γ_G expressed by Eq. (5), depends on the temperature, but not on the pressure, whereas the Lorentzian width Δ_L, given by Eq. (8), depends linearly on the sample pressure. Recent progress in the high precision spectroscopy revealed, however, that the Γ_G obtained from the line-profile analysis cannot be handled as a parameter independent of the pressure; its value decreases with increasing pressure. This is named the collisional narrowing effect, which was first discussed by Dicke [8,9]. Because of the complex effect of the collisional narrowing, we should note that the Lorentzian width is also changed.

Thus it is essential to use the generalized Voigt function for fitting the observed line profiles, where the Gaussian width is also handled as a parameter to be adjusted. By using the generalized Voigt function, Yamada and coworkers have been able to fit the line profiles successfully in the millimeter wave region [10,11] and also in the NIR region [12].

The Maxwell–Boltzmann distribution of the translational energy should be seen in the observed Gaussian width at zero pressure, where no collisional effect expected. Since it is impossible to observe any spectra at zero pressure, we have to evaluate the Gaussian width at the zero pressure limit by extrapolation from the values observed in low pressures.

3. Experimental procedure

In our recent study we have measured a ^{13}C acetylene line, $P(16)$ of the $\nu_1 + \nu_3$ band in the near-infrared (NIR) region ($\sim$1.5 μm) [7]. This transition was selected by the following reasons:

(i) large Doppler widths in NIR help to decrease the relative uncertainty of its measurement,
(ii) a high precision, comb-stabilized, NIR diode-laser spectrometer is available in our laboratory at NMIJ (AIST), which is essential for the present purpose,
(iii) acetylene is a light molecule having transitions in NIR region with reasonable intensity, and its rovibrational spectra are not too congested to find an isolated line,
(iv) since acetylene is a light molecule, its Doppler width is large, which helps to reduce the relative uncertainty of its measurement,
(v) acetylene is a non-polar molecule, and thus the collisional effects are expected to be small,
(vi) since acetylene is non-polar and stable, no special handling is required for the sample cell, and
(vii) the line center position of this particular transition of the isotope substituted acetylene is known very accurately: 194 369 569 383.6(1.3) kHz [13].

The last item is important for finding the exact mode number of the comb signal as described below.

The high precision NIR spectrometer used for the measurements is a comb-stabilized diode-laser system which is illustrated in Fig. 1. The details of the spectrometer have been published already [7]. We describe here some important remarks.

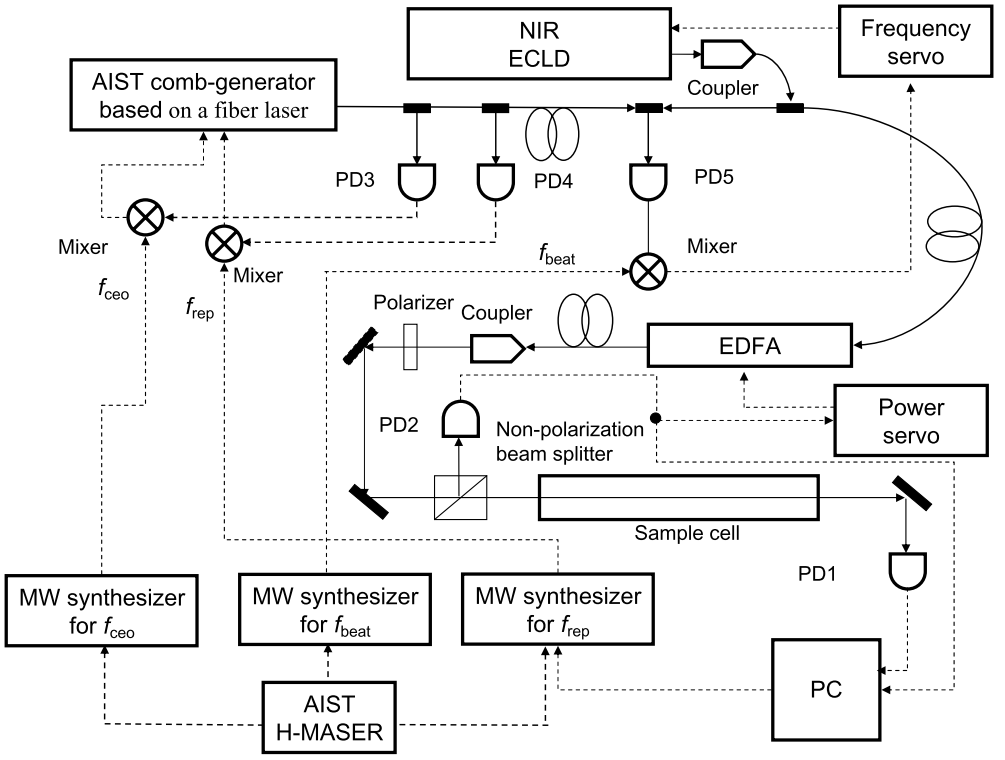

Fig. 1. The spectrometer used in the present study is illustrated schematically. Following abbreviations are used in the figure: ECLD (external cavity laser diode), PD (photodetector), EDFA (erbium-doped fiber amplifier).

The frequency of an external-cavity laser diode (ECLD) is phase-locked to a fiber-based optical frequency-comb signal, which is developed at NMIJ [14]. The frequency of the ECLD locked to the n-th mode of the comb signal is then expressed as:

$$f(n) = nf_{\mathrm{rep}} \pm f_{\mathrm{ceo}} \pm f_{\mathrm{beat}} \tag{10}$$

where, f_{rep}, f_{ceo}, and f_{beat} are the repetition frequency of the mode-locked fiber laser, the carrier-envelope-offset frequency of the fiber comb, and the frequency of the beat note between the ECLD and the comb, respectively. Because the position of the observed line is about 194 THz and the f_{rep} is about 54 MHz in the present experiment, the mode number n is a huge integer, about 3.6 million. Synthesizers are employed for frequency locking of those three frequencies, which refer to a hydrogen maser of NMIJ as the frequency standard.

In order to measure Doppler-broadened line profiles of an acetylene transition in NIR, it is required to scan the ECLD frequency over 2 GHz, in order to get information of the background radiation power. The wide scan was realized by tuning the repetition frequency ($f_{\mathrm{rep}} \approx 54$ MHz) of the comb. The phase locking of f_{rep} is achieved by controlling the cavity length of the mode-locked fiber-oscillator; mechanically by a drum-type PZT (for proportional correction), around which a part of the fiber ring-cavity of the mode-locked fiber oscillator is wound, and thermally by a Peltier device (for integral correction), which is mounted to the cavity container.

In order to measure the line profile as precise as possible, it is important to stabilize the power of the incident radiation, $I_0(\nu)$ of Eq. (1). The radiation from ECLD is amplified by a fiber-amplifier (EDFA) as shown in Fig. 1, and then emitted to the free space by a coupler. A polarizer is placed before the beam splitter to define the polarity of the radiation. The incident radiation power is monitored by a detector, PD_2, taking out a part of the power by a non-polarization beam-splitter located just before the sample cell. The signal of this detector, D_{ref}, is used to stabilize the incident radiation power by a feed-back loop controlling the gain of EDFA.

The relative short-term stability of the incident power-level attained by the servo scheme is about 10^{-4}. The time constant for the detecting system is 0.5 s and the signal was averaged over ∼3.5 s for each frequency point. The actual incident power levels directed to the sample cell were between 20 to 60 μW.

The transmitted signal, $I(\nu)$ of Eq. (1), is monitored by a detector, PD_1; the detector signal D_{sig} is proportional to $I(\nu)$. The diameter of the laser beam was about 1.3 mm in the cell.

Sealed-off-type sample cells of lengths ∼150 mm with wedged quartz windows (THORLABS Co.) were filled by the sample of $^{13}C_2H_2$, with pressures about 0.3, 1, 3, and 5 Torr (1 Torr = 133.322 Pa). Since the sample pressures in the cell were not known with high accuracy required for the present purpose, the observed intensities were used as the measure of pressure; adequacy of this procedure has been given elsewhere [6,11,15].

The cells have been installed in an air-conditioned laboratory where the all measurements have been carried out. We assume that the molecules in the cell are in thermal equilibrium. The temperature of the room was found to be fairly constant, i.e. we found

$$T_{room} = 294.65(30)\ \mathrm{K} \tag{11}$$

4. Analysis and results

The transmittance spectra $T(\nu) = I(\nu)/I_0(\nu)$ should be proportional to the ratio of the detected signals: $T'(\nu) = D_{sig}/D_{ref}$. Thus

$$T'(\nu) = \zeta T(\nu) \tag{12}$$

where ζ is a constant determined by the experimental condition. Applying Lambert–Beer's law, Eq. (1), this equation can be rewritten as

$$T'(\nu) = \zeta \exp\bigl[-\sigma V(\nu, \nu_0)\bigr] \tag{13}$$

Although the signal D_{ref} is well regulated as described above, we observed very slight fluctuation of it during a scan. In addition it may not be perfectly proportional to the incident power of radiation $I_0(\nu)$ in Eq. (1). Thus, the ζ cannot be handled as a constant in the analysis. We have employed a quadratic function of ν to express ζ, which represents the background correction:

$$\zeta(\nu) = a_0 + a_1\nu + a_2\nu^2 \tag{14}$$

where a_1 and a_2 are very small compared with a_0.

The observed line profiles have been analyzed using Eq. (13) with Eq. (14), employing a least-squares-fit procedure. Using the generalized Voigt function for the profile function $V(\nu, \nu_0)$, four parameters, the line center, the line intensity, the Gaussian width, and the Lorentzian width, have been adjusted for each profile together with three background parameters a_0, a_1, and a_2 as described in Ref. [10]. The fits were carried out directly to the observed signal $T'(\nu)$ given in Eq. (13). The quality of the fits is very good as shown in Fig. 2 for a measurement of the 0.3 Torr sample. Another example of the 1.0 Torr sample is given in Fig. 3 of our previous paper [7]. The typical uncertainty of the Gaussian width, determined from the fit was 350 ppm, and that of the intensity factor was 400 ppm.

The pressure dependence of the Lorentzian and Gaussian widths, Γ_G and Δ_L, obtained from the observed line profiles is shown in Fig. 3, where the intensity factor σ is used as a pressure scale. The collisional narrowing effect can be seen clearly there. Assuming the linear dependence of Γ_G upon pressure (i.e. intensity in the figure), its value at zero pressure was obtained employing a least-squares fit procedure (see the solid line in Fig. 3 for Γ_G), which corresponds to the Doppler width expected by the Maxwell–Boltzmann velocity distribution. The value was obtained to be $\Gamma_G = 271.29(32)$ MHz at zero pressure, where the uncertainty is given by one σ. This value agrees with the value 271.12(14) MHz calculated with the CODATA recommended value of k, at the sample temperature. Here the error of the calculated value is estimated from the uncertainty of the sample temperature given in Eq. (11).

The Lorentzian width increases with the sample pressure as shown in Fig. 3. Because the observed line profiles for the 0.3 and 1 Torr samples are almost Gaussian, the very small Lorentzian contribution was not well determined for them. Therefore, the Lorentzian widths for these pressures are estimated from those of 3 and 5 Torr samples by extrapolation assuming it to be zero at the zero-pressure limit (see the solid line in Fig. 3 for Δ_L).

The background parameters a_0, a_1, and a_2 were required to be adjusted for the spectra of the 0.3 and 1 Torr samples, whereas the quadratic parameter a_2 was set to zero for the 3 and 5 Torr spectra. Broader lines have less information for the background, and the effect of a_2 is essentially absorbed by the Lorentzian broadening.

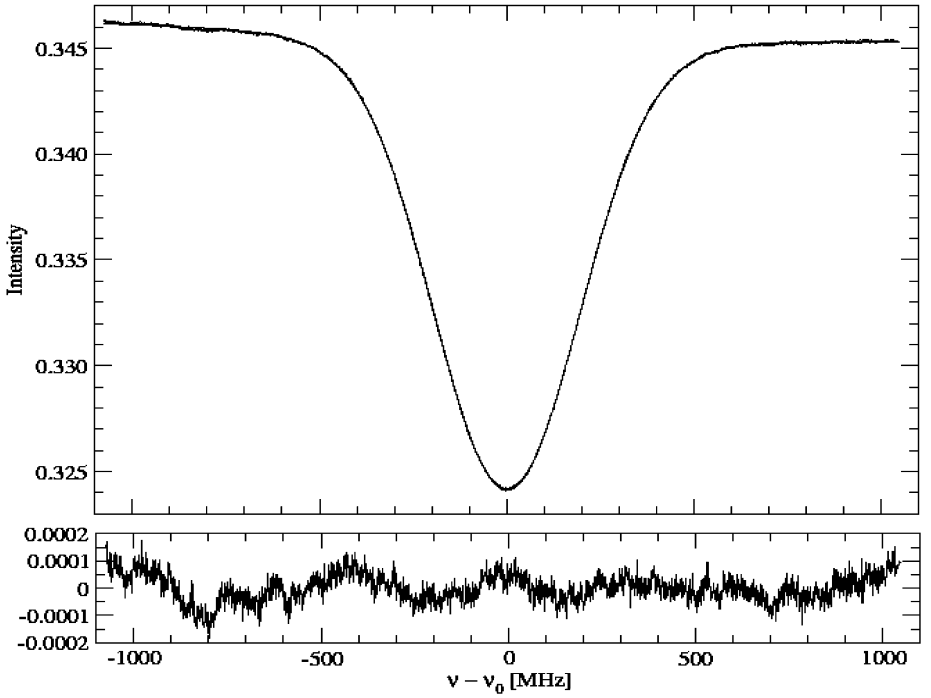

Fig. 2. An example of the observed line profile (sample pressure ≈ 0.3 Torr) is displayed by dots, together with the calculated one in solid line. The deviations, obs.—calc values, are indicated in the bottom in an expanded scale, which are otherwise hard to see because the observed profile is so well reproduced by the calculated one. The intensity axis corresponds to the value of T' defined by Eq. (13). The frequency axis is given as the difference from the exact line position, $\nu_0 = 194\,369\,569\,383.6(1.3)$ kHz [13]. The mode oder of the comb signal used for measuring this spectrum is found to be $n = 3\,602\,802$.

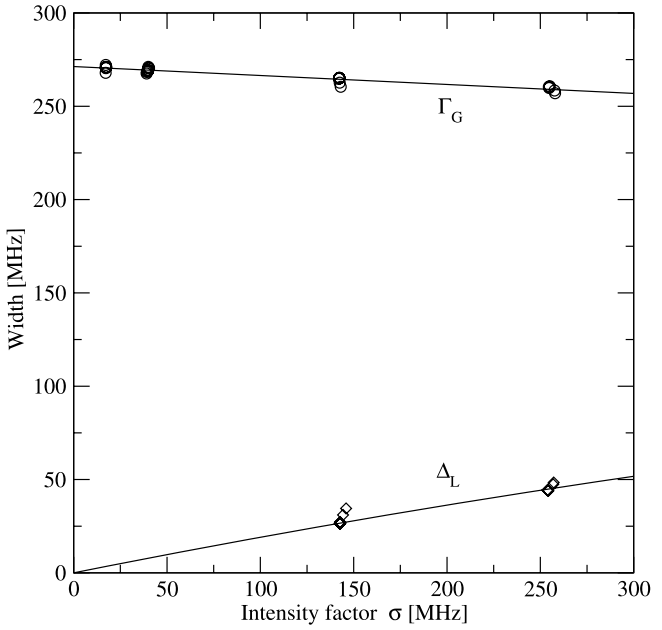

Fig. 3. The pressure dependence of the Gaussian width Γ_{G} (HWM/e) and the Lorentzian width Δ_{L} (HWHM) obtained in the present study is displayed. The intensity factor σ derived from the profile analysis is used as the pressure scale.

5. Discussion

The uncertainty of Γ_G determined for the zero-pressure limit in the present study is 1200 ppm, which is still far more inaccurate compared with the present CODATA recommended value of k. The following items may be considered to improve the accuracy in the future.

5.1. Correction for the homogeneous width

In the present analysis we have considered that the Lorentzian width (homogeneous width) is caused purely by the molecular collision. In addition to the collisional (pressure) broadening, the homogeneous width must contain contributions of the natural broadening, the power broadening, and the transit broadening. The natural broadening and the power broadening are found to be negligible for the present experimental condition: less than 1 kHz. On the other hand the transit broadening is fairly large because the beam radius of the probe laser is only 1.3 mm; we predict its contribution to the Lorentzian width to be 200 kHz at the most. However, Daussy et al. [6] reported that the transit broadening effect is absorbed in the normal Doppler effect.

The neglect of these three contributions, however, affects only a little on the resulting Gaussian width, less then the estimated uncertainty in the present case, because the Lorentzian contribution is separated from the Gaussian one by deconvolution analysis.

5.2. Correction for the probe laser linewidth

The width of the probe laser (ECLD) used in the present study is estimated to be less than 100 kHz. It may contribute, however, directly to the Gaussian width (and also to the Lorentzian width), and therefore we have to check it and improve it if necessary.

5.3. Stabilization of the sample temperature

In the present experiment, the temperature of the sample cell was not controlled. Without employing any active temperature control, the temperature distribution along the optical path can be very homogeneous in the relatively short cell used in the present study. We rely on the air-conditioned room-temperature; the fluctuation of the temperature has been observed to be about 0.3 K. This uncertainty may contribute to the error of 500 ppm, which has to be improved.

5.4. Stabilization of the incident radiation power

As mentioned in Section 4, we found that ζ (the background) in Eq. (13) is not constant. This is mainly caused by the interference fringes which are not fully corrected in our power-stabilization system. Although the effect of this was corrected in the deconvolution analysis by introducing the quadratic curve, Eq. (14), it may cause errors in the results. As the consequence, we found that the standard errors for the Gaussian widths obtained from the profile analysis are often too optimistic. Thus, for the zero-pressure extrapolation fit of the Gaussian widths, we have not employed the weighted least-squares. As stated in our earlier paper [7], we found that the zero-pressure line position obtained from the present experiment agrees with the accurate value reported by Hong et al. [13] by $-0.14(18)$ MHz within the present experimental uncertainty. However, the present uncertainty 180 kHz is much too large compared with that of Hong et al., 1.3 kHz. The large uncertainty of the present study is an indication of the error caused by the background correction. Further improvement in the stabilization of the incident radiation-power is desired. In addition, the linearity of the detector response should be an important issue to be checked.

5.5. Nature of collisional narrowing effect

In order to obtain the Doppler width at zero pressure, we assumed that the observed Gaussian width depends linearly on the sample pressure. The effect is, however, rather complicated. Wehr et al. published recently a paper on the Dicke-narrowed line shapes of CO [16], in which they stated that it was not possible to explain the observed

effect quantitatively by the mass diffusion constant. The most recent review on the collisional narrowing effect may be found in the book of Hartmann, Boulet, and Robert [17].

From the experimental point of view, it is important to find how far we can rely on the linear extrapolation to the zero pressure.

In connection with the last item given above, we would like to comment on the recent work of Casa et al. [18]: they determined the Boltzmann constant from the temperature dependence of the Gaussian width observed for a CO_2 line in a NIR band measured with the constant density condition. As reported by Hikida et al. [12] for another NIR band of CO_2, significant collisional narrowing is expected for the transitions of CO_2 in NIR for the pressures employed in their experiments. Therefore, it may be worth checking carefully the temperature dependence of the collisional narrowing effect in the condition of constant density, theoretically and/or experimentally.

As a conclusion, the Doppler width, Γ_G, was determined in the present study for C_2H_2 from the NIR spectra with the uncertainty of 1200 ppm. Because we did not measure the temperature accurately, the Boltzmann constant derived from it, $k = 1.3940(17)\ \mathrm{J\,K^{-1}}$, is considerably less accurate than the presently recommended CODATA value [1,2].

Acknowledgements

We would like to express our thanks to Prof. H. Matsumoto, Dr. Y. Nakajima, and Dr. F. Ito for the help during the course of the work.

References

[1] P.J. Mohr, B.N. Taylor, D.B. Newell, Rev. Mod. Phys. 80 (2008) 633–730; simultaneously also: J. Phys. Chem. Ref. Data 37 (2008) 1187–1284.
[2] P.J. Mohr, B.N. Taylor, Rev. Mod. Phys. 77 (2005) 1–107.
[3] I.M. Mills, P.J. Mohr, T.J. Quinn, B.N. Taylor, E.R. Williams, Metrologia 43 (2006) 227–246.
[4] C.J. Bordé, C. R. Physique 5 (2004) 813–820.
[5] C.J. Bordé, Philos. Trans. R. Soc. London A 363 (2005) 2177–2201.
[6] C. Daussy, M. Guinet, A. Amy-Klein, Y. Djerroud, K. Hermier, S. Briaudeau, C.J. Bordé, C. Chardonnet, Phys. Rev. Lett. 98 (2007) 250801-4.
[7] K.M.T. Yamada, A. Onae, F.-L. Hong, H. Inaba, H. Matsumoto, Y. Nakajima, F. Ito, T. Shimizu, J. Mol. Spectrosc. 249 (2008) 95–99.
[8] R.H. Dicke, Phys. Rev. 89 (1953) 472–473.
[9] P.L. Varghese, R.K. Hanson, Appl. Opt. 23 (1984) 2376–2385.
[10] K.M.T. Yamada, H. Abe, J. Mol. Spectrosc. 217 (2002) 87–92.
[11] I. Morino, K.M.T. Yamada, J. Mol. Spectrosc. 233 (2005) 77–85.
[12] T. Hikida, K.M.T. Yamada, M. Fukabori, T. Aoki, T. Watanabe, J. Mol. Spectrosc. 232 (2005) 202–212.
[13] F.-L. Hong, A. Onae, J. Jiang, R. Guo, H. Inaba, K. Minoshima, T.R. Schibli, H. Matsumoto, K. Nakagawa, Opt. Lett. 28 (2003) 2324–2326.
[14] H. Inaba, Y. Daimon, F.-L. Hong, A. Onae, K. Minoshima, T.R. Schibli, H. Matsumoto, M. Hirano, T. Okuno, M. Onishi, M. Nakazawa, Opt. Express 14 (2006) 5223–5231.
[15] T. Hikida, K.M.T. Yamada, J. Mol. Spectrosc. 239 (2006) 154–159.
[16] R. Wehr, R. Ciurylo, A. Vitcu, F. Thibault, J.R. Drummond, A.D. May, J. Mol. Spectrosc. 235 (2006) 54–68.
[17] J.-M. Hartmann, C. Boulet, D. Robert, Collisional Effect on Molecular Spectra, Elsevier, Amsterdam, 2008.
[18] G. Casa, A. Castrillo, G. Galzerano, R. Wehr, A. Merlone, D. Di Serafino, P. Laporta, L. Gianfrani, Phys. Rev. Lett. 100 (2008) 200801-4.